In situ spectroellipsometric study of the nucleation and growth of amorphous silicon

A. Canillas, E. Bertran, and J. L. Andújar
Departament de Fisica Aplicada i Electrònica, Universitat de Barcelona, Avinguda Diagonal, 645, 08028 Barcelona, Spain

B. Drévillon
Laboratoire de Physique des Interfaces et des Couches Minces (UPR A258 du CNRS) Ecole Polytechnique, 91128 Palaiseau, France

(Received 9 April 1990; accepted for publication 16 May 1990)

A detailed *in situ* spectroellipsometric analysis of the nucleation and growth of hydrogenated amorphous silicon (*a*:Si:H) is presented. Photoelectronic quality *a*-Si:H films are deposited by plasma-enhanced chemical vapor deposition on smooth metal (NiCr alloy) and crystalline silicon (*c*-Si) substrates. The deposition of *a*-Si:H is analyzed from the first monolayer up to a final thickness of 1.2 μm. In order to perform an improved analysis, real time ellipsometric trajectories are recorded, using fixed preparation conditions, at various photon energies ranging from 2.2 to 3.6 eV. The advantage of using such a spectroscopic experimental procedure is underlined. New insights into the nucleation and growth mechanisms of *a*-Si:H are obtained. The nucleation mechanism on metal and *c*-Si substrates is very accurately described assuming a columnar microstructural development during the early stage of the growth. Then, as a consequence of the incomplete coalescence of the initial nuclei, a surface roughness at the 10–15 Å scale is identified during the further growth of *a*-Si:H on both substrates. The bulk *a*-Si:H grows homogeneously beneath the surface roughness. Finally, an increase of the surface roughness is evidenced during the long term growth of *a*-Si:H. However, the nature of the substrate influenced the film growth. In particular, the film thickness involved in the nucleation-coalescence phase is found lower in the case of *c*-Si (67 ± 8 Å) as compared to NiCr (118 ± 22 Å). Likewise films deposited on *c*-Si present a smaller surface roughness even if thick samples are considered (> 1 μm). More generally, the present study illustrates the capability of *in situ* spectroellipsometry to precisely analyze fundamental processes in thin-film growth, but also to monitor the preparation of complex structures on a few monolayers scale.

I. INTRODUCTION

A detailed knowledge of the growth mechanisms of hydrogenated amorphous silicon (*a*-Si:H) is of considerable interest from a fundamental point of view and also for improving device performances. However the more conventional *in situ* surface probes are incompatible with the plasma-enhanced chemical vapor deposition (PECVD) generally used to prepare photoelectronic quality *a*-Si:H. On the contrary, when coupled to a plasma chamber, spectroellipsometry is a nondestructive technique which does not perturb the growth processes. *In situ* ellipsometry has proved very powerful in analyzing the evolution of *a*-Si:H microstructure during growth.[1-3] *In situ* ellipsometry at fixed wavelength, combined with the fast time resolution provided by the photoelastic modulation, is particularly well adapted to perform detailed kinetic studies of *a*-Si:H.[2-6] Moreover the spectroscopic facility allows precise descriptions of the film morphology evolution.

The previous spectroellipsometry experiments revealed that the growth of *a*-Si:H is influenced by the deposition conditions and the nature of the substrate. In particular, transparent conducting oxide and glass substrates were found to be reduced by the silane plasma during the early stage of the growth.[5,6] In contrast, a nucleation mechanism was observed when depositing *a*-Si:H, from a rf discharge, on metallic or crystalline silicon (*c*-Si) substrates.[4,5,7] In the case of metallic substrates, optical models based on hemispherical nucleation were used to qualitatively reproduce the shape of the real time trajectories.[4] A surface roughness, at the 10–50 Å scale, is then generally observed during the bulk *a*-Si:H growth. Using metallic substrates, the presence of this surface roughness was attributed to the incomplete coalescence of the initial nuclei.[4] As a matter of fact, the thickness of the surface roughness was found roughly equal to the internuclei distance.[4] Such a growth model, displayed in Fig. 1, qualitatively reproduces the behavior of the ellipsometric trajectories up to a final thickness of 1000 Å.[4] The presence of a strong ion bombardment during growth induces the complete coalescence of the nuclei.[3] Under these extreme deposition conditions, generally incompatible with the preparation of photoelectronic quality *a*-Si:H, the film surface roughness disappears.[3,8] More recently, the growth of *a*-Si:H on *c*-Si and metal were carefully compared in a kinetic ellipsometry experiment performed at a single photon energy (3.4 eV).[9] The nucleation of *a*-Si:H on metal was found consistent with an hemispherical nucleation model while the nucleation on *c*-Si was described using a cylindrical geometry.[9]

This paper describes the results of a detailed study of the

 0021-8979/90/182752-08$03.00

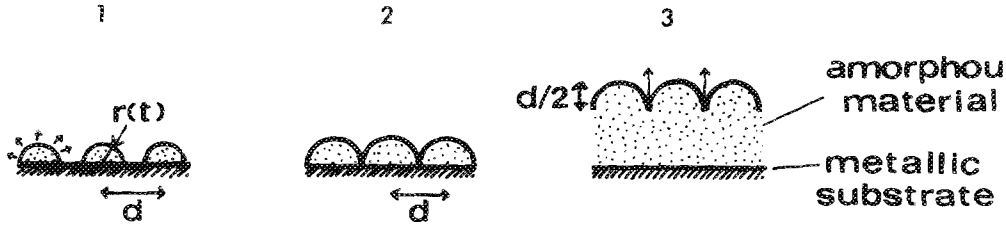

FIG. 1. Schematic representation of the nucleation and growth model assuming a constant surface roughness.

nucleation and growth of photoelectronic quality *a*-Si:H deposited by PECVD on smooth, homogeneous metal and *c*-Si substrates. In order to perform an improved analysis of the growth mechanism, real time ellipsometric trajectories are recorded, using fixed preparation conditions, at various photon energies ranging from 2.2 to 3.6 eV. The present study gives new insights into the nucleation-coalescence mechanism of *a*-Si:H. Furthermore, it allows a precise description of the *a*-Si:H growth from the deposition of the first monolayers up to a final thickness of more than 1 μm. More generally, this analysis illustrates the capability of *in situ* spectroellipsometry to analyze fundamental processes and to monitor the growth of complex structures on a few monolayers scale.

II. EXPERIMENTAL DETAILS

A capacitively coupled conventional glow-discharge reactor operating at 13.56 MHz was used for deposition of photoelectronic quality *a*-Si:H films.[10] The substrates were placed on the grounded anode, the anode-to-cathode distance being fixed to about 40 mm. The reactor was always evacuated down to a base pressure of the order of 10^{-4} Pa. The substrate temperature was fixed to 300 °C. The standard deposition conditions were fixed as follows: pure silane with a total pressure of 20 Pa and 30 sccm flow rate, rf power of 20 W. The average deposition rate estimated from kinetic ellipsometry measurements was: 1.45 ± 0.15 Å s^{-1}. The *a*-Si:H films were deposited on metal and *c*-Si covered with native oxides. Metallic substrates consist of NiCr 400-Å thick films evaporated at 250 °C on glass. During the plasma ignition procedure, the substrate is isolated from the discharge by an automatic shutter. Thus real time ellipsometry data acquisition is started after plasma stabilization.

Two fused silica windows allow the reflection on the substrate of the beam of a fast spectroscopic phase modulated ellipsometer (SPME) described in detail elsewhere,[11,12] with an angle of incidence of 69.5°. Let us briefly recall that spectroellipsometry measures, as a function of the photon energy, the complex ratio between the parallel (p) and perpendicular (s) reflection coefficients of the electric field $\rho = r_p/r_s = \tan\Psi \exp(i\Delta)$. In the case of a homogeneous material with a sharp interface with ambient, ρ is directly related to the dielectric function of the sample $\epsilon = \epsilon_1 + i\epsilon_2$, otherwise a multilayer calculation is necessary.[13] For kinetic studies, the photon energy was fixed and N points ρ_i were recorded at regular intervals Δt. Various photon energies ranging from 2.25 to 3.54 eV were used corresponding to a light penetration in *a*-Si:H decreasing from a few thousand angstroms to about 100 Å. As a consequence the ellipsometric measurements were integrated during variable time intervals ranging from 0.5 s (UV light) up to 1.5 s (2.25 eV), each individual real time trajectory corresponding typically to $N = 3000$ points. The experimental conditions corresponding to the various kinetic ellipsometry trajectories are summarized in Table I.

The experimental (Ψ,Δ) trajectories will be systematically compared to some theoretical computations based on various types of nucleation and growth models. In the models described below, the index of a substrate is deduced from the ellipsometric measurement performed immediately before the *a*-Si:H growth. The refractive index of the bulk *a*-Si:H corresponds to the value determined by fitting the real time trajectory to the growth model assuming a constant surface roughness (see Fig. 1).[4] The index of the mixed layers are the result of a Bruggeman effective medium approximation (EMA) assuming spherical or cylindrical inclusions.[14,15]

III. EXPERIMENTAL RESULTS

A. Nucleation of *a*-Si:H

The nucleation models are displayed in Fig. 2. The most simple assumption corresponds to the uniform growth of a homogeneous material with a constant index. In the hemispherical nucleation model, a hexagonal network of hemispherical nuclei of *a*-Si:H is created with an average distance d between them. The radius of the nuclei increases continuously until the hemispheres come into contact. It results in a density deficient layer of growing thickness, the void volume fraction of the film decreasing from $f = 1$ down to 0.39. The index of this layer is continuously deduced from an EMA

TABLE I. Experimental conditions corresponding to the various ellipsometric trajectories. In each case, the kinetic trajectory is fitted to the growth models up to a final thickness d_{tot}.

Substrate	E (eV)	v_d (Å s^{-1})	d_{tot} (Å)	P_{tot} (Pa)	Power (W)
NiCr	3.54	1.45	600	20	20
NiCr	3.40	1.45	600	20	20
NiCr	3.10	1.45	800	20	20
NiCr	2.82	1.45	1000	20	20
NiCr	2.70	1.45	2000	20	20
NiCr	2.48	1.45	3000	20	20
NiCr	2.25	1.45	4500	20	20
c-Si	3.40	0.50	500	10	10
c-Si	3.40	2.50	650	30	10
c-Si	3.40	1.40	650	20	20

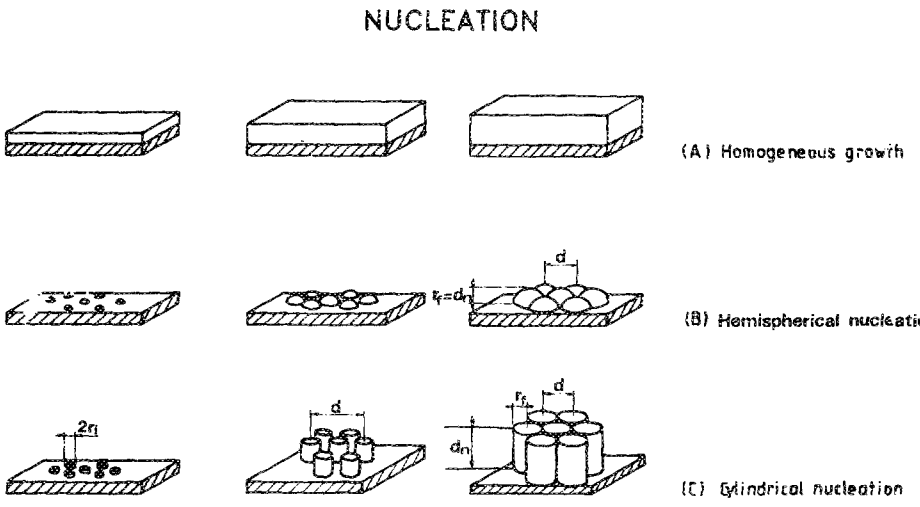

FIG. 2. Schematic representation of the nucleation models.

calculation.[4,16] In a different way, the third model assumes a columnar microstructural development during the nucleation phase.[9] In this latter case, the *a*-Si:H nuclei are located on a hexagonal network separated by an average distance $d = 60$ Å. In d being fixed, the free parameters of this last model are the initial and final radii r_i and r_f and the final cylinder height d_n.

The real time trajectories recorded at 3.1 and 3.54 eV during the deposition of *a*-Si:H on NiCr substrates are compared in Figs. 3(a) and 3(b) to the nucleation models described above. In both cases, the experimental trajectories strongly depart from the uniform growth assumption (long dashes) confirming previous results.[4,5,7] In contrast the (Ψ,Δ) SPME trajectory, recorded at 3.1 eV [Fig. 3(a)] is in rather good agreement with the hemispherical nucleation assumption corresponding to $d = 80$ Å (short dashes). A similar conclusion was recently deduced from an ellipsometric study at 3.4 eV of the early stage of the growth of *a*-Si:H on Mo and Cr substrates.[9] Nevertheless, the experimental results obtained at 3.54 eV [Fig. 3(b)] can rule out the hemispherical nucleation model. At 3.54 eV the experimental trajectory is only compatible with the columnar nucleation model, a very good fit with the cylindrical nucleation also being obtained at 3.1 eV (solid lines). The fitted three parameter values r_i,r_f, and d_n are presented, as functions of the photon energy, in Table II. Compatible values are obtained from 2.25 to 3.54 eV evidencing the validity of the columnar model to account for the nucleation phase. In the case of a metallic substrate, the following average values can

TABLE II. Structural parameters related to the nucleation and coalescence phases.

Substrate	E (eV)	r_i (Å)	r_f (Å)	f_{ti}	d_n (Å)	d_c (Å)	α
NiCr	3.54	22	30	0.1	72	40	1
NiCr	3.40	22	30	0.1	55	55	1
NiCr	3.10	19	28	0.2	50	75	1
NiCr	2.82	16	28	0.2	42	65	1
NiCr	2.70	20	28	0.2	72	40	1
NiCr	2.48	18	28	0.2	85	55	1
NiCr	2.25	22	28	0.2	60	60	1
c-Si	3.40	26	29	0.15	33	30	0.3
c-Si	3.40	25	29	0.26	34	30	0.5
c-Si	3.40	26	30	0.10	35	40	0.3

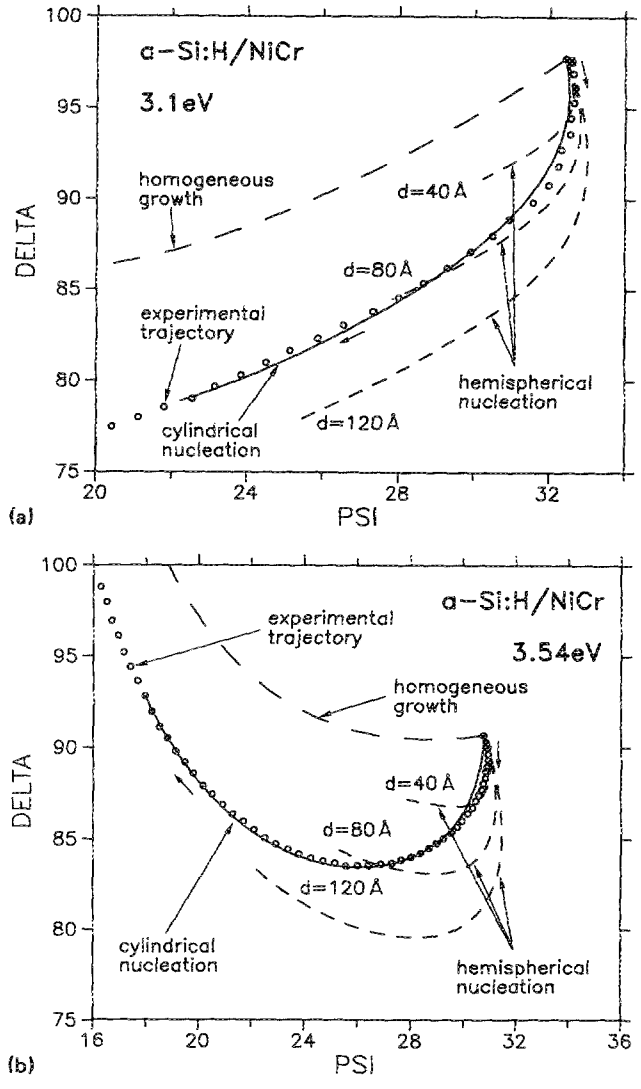

FIG. 3. Real time examinations of the beginning of the growth of *a*-Si:H on NiCr substrate, (a) at 3.1 eV; (b) at 3.54 eV.

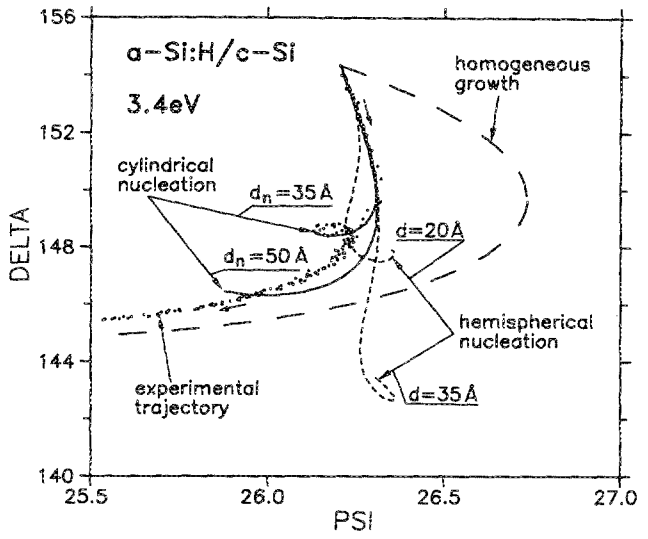

FIG. 4. Real time examination, at 3.40 eV, of the beginning of the growth of *a*-Si:H deposited in standard conditions on *c*-Si substrate.

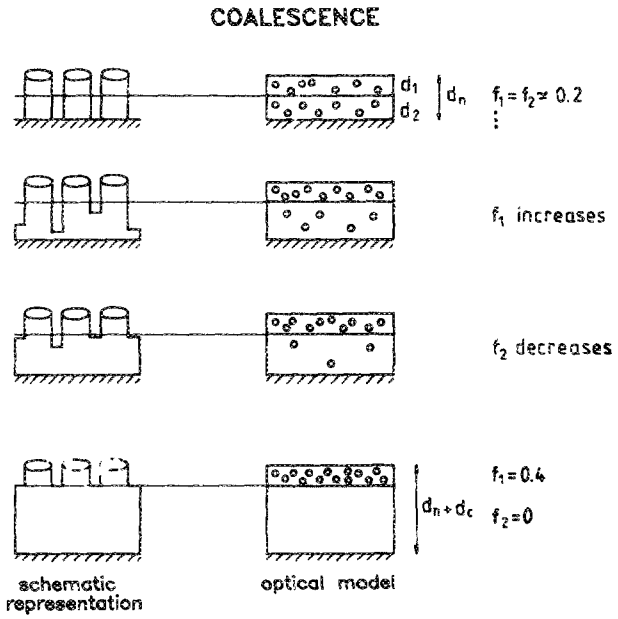

FIG. 5. Schematic representation of the coalescence model.

be estimated from the spectroscopic data: $r_i = 20 \pm 4$ Å; $r_f = 29 \pm 1$ Å, and $d_n = 60 \pm 20$ Å. The high r_f value shows that the cylinders almost come into contact at the end of the nucleation phase.

The beginning of the growth of *a*-Si:H deposited on *c*-Si substrate, recorded at 3.4 eV, is displayed in Fig. 4. Figures 3 and 4 correspond to similar preparation conditions. The experimental (Ψ,Δ) trajectory of Fig. 4 describes a well-defined loop. By contrast, a "lobe and cusp" behavior is observed in the rotating analyzer ellipsometry measurements.[1,7] This apparent difference of the ellipsometric trajectory shapes can probably be attributed to the best time resolution provided by the SPME technique. As already pointed out, the experimental (Ψ,Δ) trajectory, shown in Fig. 4, clearly departs from the uniform growth and the hemispherical nucleation assumptions.[5] In contrast, the first few seconds of the growth, and the first part of the loop are in very good agreement with the columnar nucleation assumption, confirming the conclusion of a previous ellipsometric experiment.[9] Moreover, the results of Table II show that the nucleation phase on *c*-Si substrate is very weakly affected by variations of the preparation conditions. Then, as a first conclusion it can be inferred that similar nucleation mechanisms are observed in the early stage of the growth of *a*-Si:H on *c*-Si and metal substrates. However lower values of d_n (35 Å) and larger values of r_i (26 Å) are obtained on *c*-Si, as compared to the NiCr substrate.

B. Coalescence and bulk *a*-Si:H growth

The remaining problem is the optical description of the coalescence of the initial columnar microstructure, the presence of a small roughness at the top surface of *a*-Si:H being well established.[1-4] The schematic coalescence model is shown in Fig. 5. The presence of two layers with different thickness (d_1,d_2) and void volume fractions (f_1,f_2) is considered. The refractive index of these two layers are continuously deduced from EMA calculations. At the end of the nucleation phase, the value of f_1 and f_2 is deduced from the void volume fraction of the columnar layer, thus at this initial point of the coalescence: $d_{1i} + d_{2i} = d_n$ and $f_{1i} = f_{2i} = 0.1$–0.2. The overlayer thickness d_1 is fixed during the further growth while d_2 increases linearly following the deposition rate. The value of d_1 corresponds to the result of the fit to the overall trajectory of the constant surface roughness growth model assuming a void volume fraction $f_1 = 0.39$ (see Fig. 1). The d_c represents the equivalent thickness of the coalescence phase. At the end of the coalescence phase: $d_1 + d_2 = d_n + d_c$. During this phase, the relative bulk void volume fraction f_2 decreases down to 0 while f_1 increases up to 0.39 which correspond to the constant surface roughness *a*-Si:H growth model (Fig. 1). During the coalescence, the value of f_1 as a function of the total film thickness $x(d_n < x < d_n + d_c)$ is deduced assuming the following dependence:

$$f_1 = f_{1i} + (f_{1f} - f_{1i})[(x - d_n)/d_c]^{\alpha}. \quad (1)$$

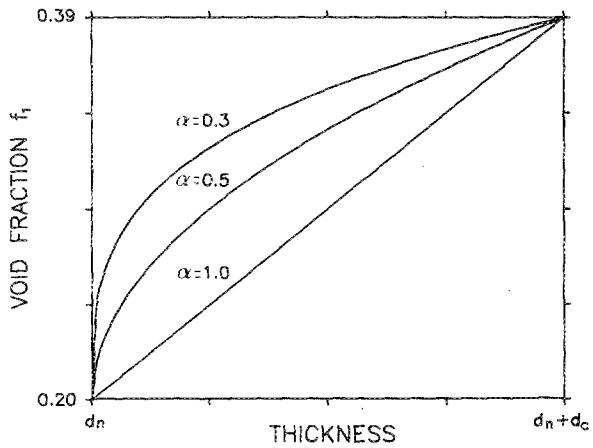

FIG. 6. Influence of the parameter α on the evolution of the overlayer void volume fraction f_1 during the coalescence period.

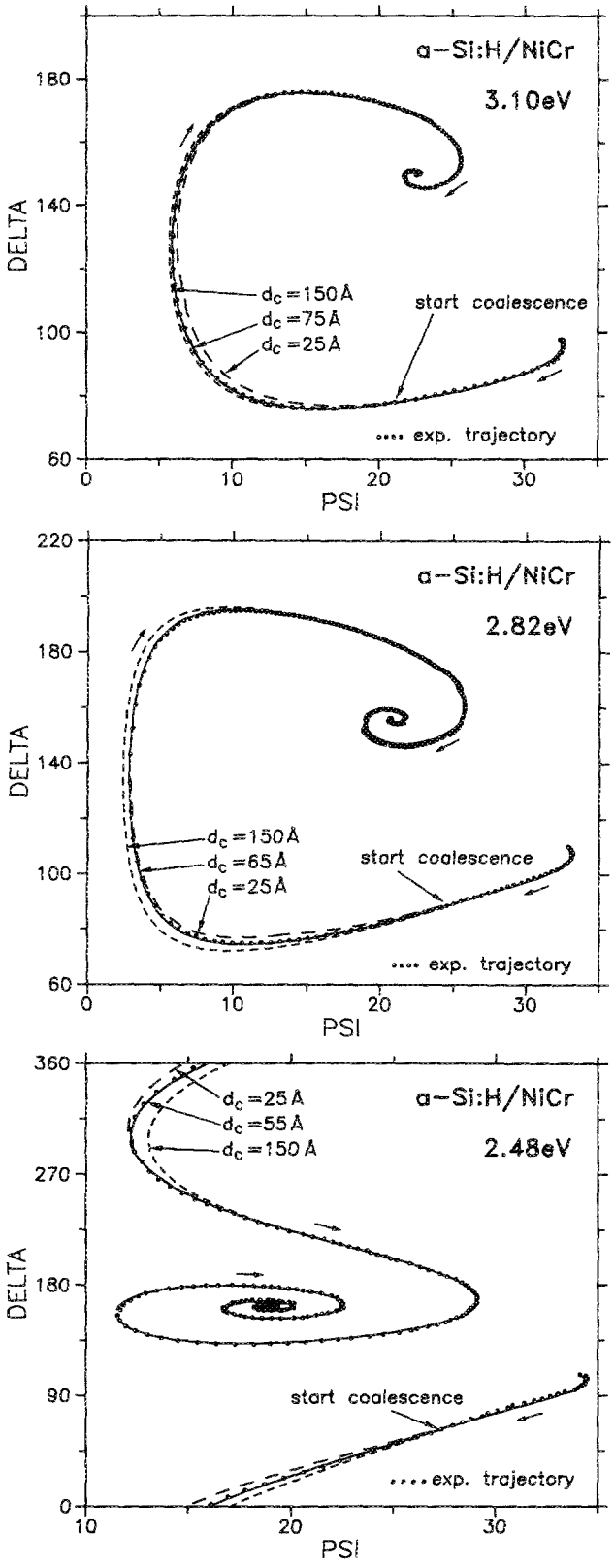

FIG. 7. Real time examinations of the long term growth *a*-Si:H deposited in standard conditions on NiCr substrate, (a) at 3.1 eV, (b) at 2.82 eV, and (c) at 2.48 eV. The dashed lines illustrate the influence of the parameter d_c on the coalescence phase.

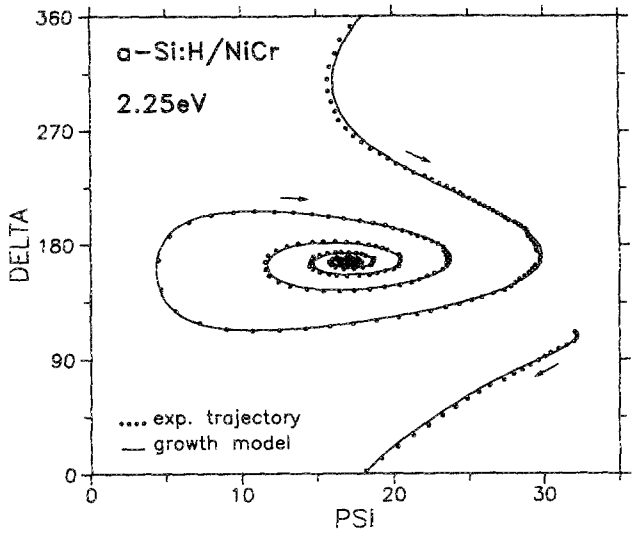

FIG. 8. Real time examination, at 2.25 eV, of the long term growth of *a*-Si:H on NiCr substrate.

The condition of a fixed material flux impinging onto the substrate during growth implies the variation of f_2 as a function of x. The value of the exponent α is related to the coalescence kinetics. In particular the values such as $\alpha < 1$ correspond to a fast increase of the overlayer void volume fraction f_1 (and consequently a fast decrease of f_2 towards 0), as shown in Fig. 6. After the end of the coalescence phase, the growth models shown in Figs. 1 and 5 are equivalent.

The coalescence model described above has been compared to the experimental trajectories recorded, at various photon energies, during the deposition of 800–4500 Å thick *a*-Si:H on NiCr substrates. The results are displayed in Figs. 7 and 8. An extremely good agreement is obtained with the growth model displayed in Fig. 5, whatever the photon energy. In particular, Figs. 8(a)–(c) illustrate the influence of the parameter d_c on the fit, in the case of a linear decrease of f_1 during the coalescence ($\alpha = 1$). The precision on the value of d_c can be estimated from Fig. 7 to about 25 Å at a fixed wavelength. The beginning of the coalescence phase is indicated on each (Ψ,Δ) trajectory displayed in Fig. 7. Finally in the case of metallic substrate, the following average value can be estimated from the spectroscopic data recorded in Table II: $d_c = (60 \pm 20)$Å.

Because of the presence of a well-defined loop in the experimental (Ψ,Δ) trajectory at the end of the nucleation phase (see Fig. 4), the data recorded in the case of the *c*-Si substrate are very sensitive to the coalescence mechanism of *a*-Si:H. Thus a slight modification of the simple coalescence model presented in Fig. 5 is necessary to fit the (Ψ,Δ) trajectory corresponding to the *c*-Si substrate. The good fit of the loop displayed in Fig. 9 is obtained when taking into account a slight increase (0.1–0.2 Å) of the cylinder radii at fixed height d_n, before the coalescence phase. Further, Fig. 9 illustrates the influence of the value of the exponent α defined by Eq. (1) on the fit. The results presented in Table II show that α and d_c are weakly affected by the preparation conditions, one obtains for the *c*-Si substrate: $\alpha = (0.4 \pm 0.1)$ and $d_c = (35 \pm 5)$ Å. A comparison between the results obtained with the two different substrates reveal a slight reduction of d_c and a significant decrease of α in the case of *c*-Si. This behavior can be interpreted as a fast coalescence in this last case.

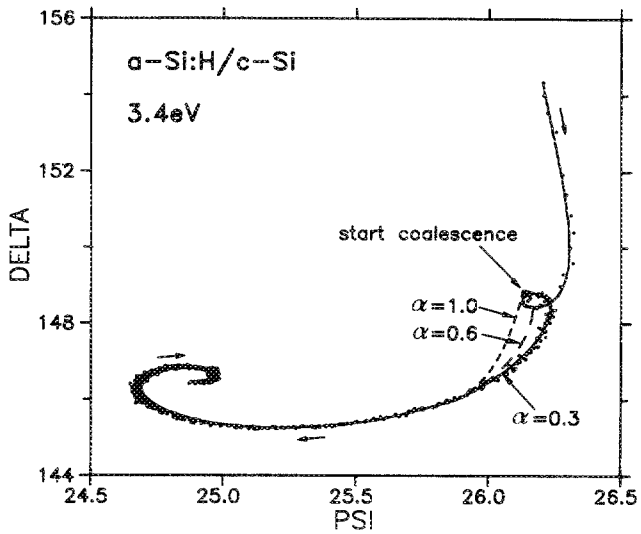

FIG. 9. Real time examination, at 3.40 eV, of the long term growth of *a*-Si:H on *c*-Si substrate. The dashed lines illustrate the influence of the parameter α on the coalescence phase.

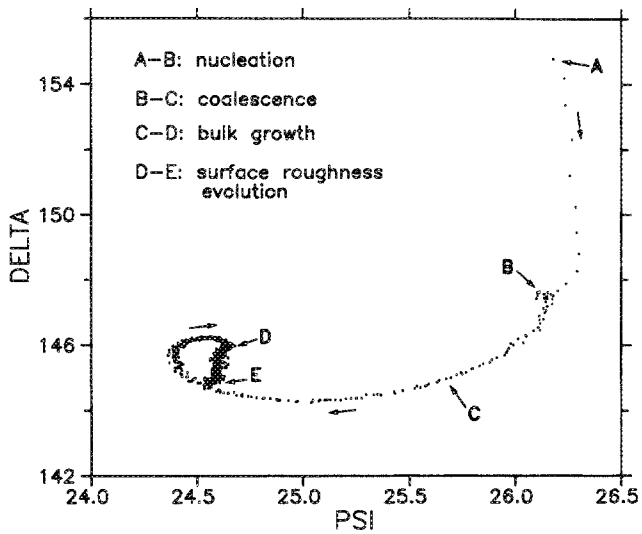

FIG. 11. Real time examination, at 3.40 eV, of the deposition of *a*-Si:H (at 10 W and 30 Pa) on *c*-Si substrate with identification of the various growth phases.

C. Evolution of the surface roughness

As already pointed out, the pseudodielectric function ϵ of *a*-Si:H can be estimated from the spectroellipsometric data by assuming a sharp interface with ambient. The long term evolutions of the imaginary part ϵ_2, obtained with NiCr substrates, are presented in Fig. 10. A slight decrease of the spectrum together with a slight shift towards lower energies are observed. This behavior is characteristic of an increase of the surface roughness with increasing film thickness.[1–3] In the same way, a continuous shift of the convergence point of the (Ψ,Δ) trajectory is observed when depositing *a*-Si:H on *c*-Si substrate (region D-E in Fig. 11). This shift can be interpreted as a surface roughness evolution during film growth. Using this assumption, the increase of the surface roughness can be estimated to be 5–10 Å for an increase in thickness of 1.0 μm at low deposition rates (less than 3 Å s^{-1}). In particular, for the standard conditions, the increase of surface roughness is estimated to 6 Å. Likewise a 3–4 Å increase of the surface roughness was observed in a previous experiment.[17]

Furthermore the comparison of the ϵ_2 spectra corresponding to the thicker films (1.2 μm) in Fig. 12 reveals a larger surface roughness in the case of the NiCr substrate. This surface roughness difference can also be estimated by the fit of the kinetic trajectories to the constant surface roughness model (displayed in Fig. 1) if the total film thickness is such that the surface roughness evolution can be neglected. In this way, the surface roughness thickness can be estimated to (14 ± 2) Å during the growth of the first 3–

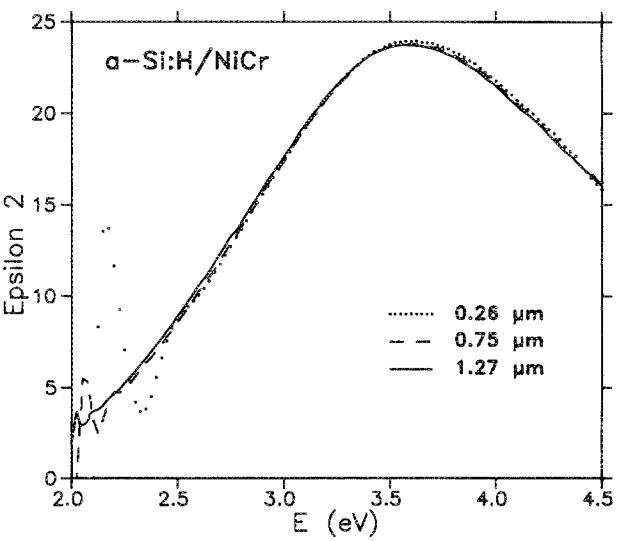

FIG. 10. Spectroellipsometric measurements corresponding to three *a*-Si:H films with different thicknesses deposited on NiCr substrates; the measurements being performed at room temperature.

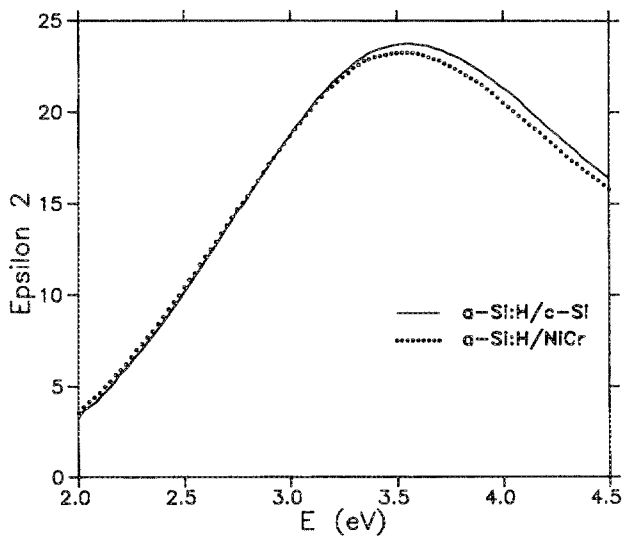

FIG. 12. Spectroellipsometric measurements on 1.2 μm thick *a*-Si:H samples deposited in standard conditions on *c*-Si and NiCr substrates; the measurements being recorded at deposition temperature.

4000 Å *a*-Si:H on NiCr, a slightly lower value being obtained in the case of *c*-Si.

IV. DISCUSSION

The present study is focused on the nucleation and growth of *a*-Si:H, prepared by PECVD, on smooth homogeneous substrates which do not lead to a chemical interaction with the silane plasma (or the *a*-Si:H film) during the deposition of the first few monolayers. However in the case of metallic substrates, a nucleation mechanism in the early stage of the growth and the presence of a roughness at the free surface during the further growth were established by *in situ* ellipsometry a few years ago.[8] Likewise, previous studies revealed the presence of a nucleation mechanism during the early stage of the growth of *a*-Si:H on *c*-Si.[4,7] These previous ellipsometric studies generally consist of the analysis of real time ellipsometric trajectories recorded at only one[1,7] or two[4,8] photon energies. Moreover very simple optical models were sometimes used. For instance, the nucleation-coalescence mechanism of *a*-Si:H was often described by a linear decrease of the void volume fraction with increasing film thickness deposition.[1,5,7] Although this approach to fitting allows one to parametrize some real time trajectories, it is not informative from a fundamental point of view.

In contrast, the present study of the growth of *a*-Si:H on the NiCr substrate is based on a set of seven real time trajectories recorded at various photon energies, each individual trajectory consisting of about 3000 (Ψ,Δ) measurements. By varying the photon energy, the light can probe different film thicknesses. Furthermore the spectroscopic analysis allows a precise description of the deposition mechanisms, in particular the growth model and the free parameters values must be independent of the wavelength of the light. Let us recall for example that, in the case of the metallic substrate, the data recorded at 3.1 eV are compatible with two different nucleation mechanisms. However, the same fit performed at different photon energies allows to rule out the hemispherical nucleation model (see Fig. 3). In the present experiment the various trajectories were recorded independently. Therefore, some discrepancies between the fitted parameters at different wavelengths of Table II can be partly attributed to an incomplete reproducibility of the preparation conditions from run to run. A better experimental system would allow simultaneously recording of several real time trajectories. Thus an improvement of the *in situ* spectroellipsometry analysis can be expected from a new device which combines the fast data acquisition of the phase modulated technique and the real time spectroscopic facility.[18]

The present study reveals that the nucleation mechanism on NiCr and *c*-Si substrates is accurately described assuming a columnar microstructural development during the early stages of the growth of *a*-Si:H. The disklike geometry corresponding to the deposition of the first monolayers can probably be understood from a thermodynamic standpoint, as already suggested.[9] In the two cases substrate/oxide/*a*-Si:H considered here, the sum of the *a*-Si:H surface and the oxide/*a*-Si:H interfacial free energies must be less than the oxide surface energy. Thus the free energy of the system is minimized by a two-dimensional growth process that maximizes interface area. Then, as a consequence of the incomplete coalescence of the initial nuclei, a surface roughness on a 10–15 Å scale can be identified during the further growth of *a*-Si:H on both surfaces. Finally, an increase of this surface roughness is evidenced when dealing with the deposition of rather thick films. This growth mechanism is found to be little affected by the preparation conditions (see Table II). The identification on the real time trajectories of these four stages of the growth can have important practical consequences for growth monitoring. In particular, because the index of *a*-Si:H is close to the value corresponding to *c*-Si, small amplitude variations of Ψ and Δ are observed during the real time evolution. As a consequence the four stages described above can very clearly identified in Fig. 11.

Nevertheless, although the same nucleation and growth model can account for the deposition of *a*-Si:H on both substrates, the results presented in Table II and the behavior displayed in Fig. 12 reveal a slight influence of the nature of the substrate on the film growth even if 1.2-μm thick samples are considered. Furthermore, the nuclei density being fixed to the same value in both cases ($d = 60$ Å), the values shown in Table II are very sensitive to relative behaviors. The film thickness involved in the nucleation-coalescence phase is found to be lower in the case of *c*-Si: 67 ± 8 Å as compared to NiCr: 118 ± 22 Å. The initial surface coverage for *c*-Si: $r_i = 26 \pm 1$ Å is slightly larger than for NiCr: $r_i = 20 \pm 4$ Å. Moreover, in the *c*-Si case the exponent α defined by Eq. (1) is found to be 0.4 ± 0.1, indicating a faster coalescence kinetic process than in the NiCr case. In summary, these results show that the growth of *a*-Si:H on NiCr departs more clearly from the uniform behavior, this substrate corresponding further to the more sensitive surface roughness (see Fig. 12). These behaviors can probably be attributed to different substrate surface morphologies, the NiCr film evaporated on glass probably being less smooth than the *c*-Si substrate. In the same way, the *a*-Si:H surface roughness is partly related to the substrate morphology. This last trend was clearly identified when depositing *a*-Si:H on rough substrates like transparent conducting oxides.[6] This strong influence of the substrate was attributed to the low surface diffusion length of the precursors of *a*-Si:H.[3,9]

V. SUMMARY AND CONCLUSIONS

We have presented a detailed *in situ* spectroellipsometry analysis of the nucleation and growth of photoelectronic quality *a*-Si:H deposited on smooth metal and crystalline silicon (*c*-Si) substrates. As compared to the previous *in situ* ellipsometric experiments, various kinetic real time trajectories recorded at different photon energies, using similar preparation conditions, have been used in the present study. The advantage of using such a spectroscopic experimental procedure has been underlined. New insights into the nucleation and growth mechanisms of *a*-Si:H have been obtained. The present study reveals that the nucleation mechanism on metal and *c*-Si substrates is accurately described assuming a columnar microstructural development during the early stages of the growth of *a*-Si:H. Then, as a consequence of the incomplete coalescence of the initial nuclei, a slight surface roughness is identified during the further

growth of *a*-Si:H on both substrates while the bulk *a*-Si:H grows homogeneously beneath this surface roughness. Finally, an increase of the surface roughness is evidenced when dealing with the deposition of thick films. However, the nature of the substrate influenced the film thickness involved in the nucleation-coalescence phase is found to be lower in the case of *c*-Si: 67 ± 8 Å as compared to NiCr: 118 ± 22 Å. More generally, the growth of *a*-Si:H on NiCr departs more clearly from the uniform behavior.

Finally the present study illustrates the capability of *in situ* spectroellipsometry to provide a very precise description of a thin-film growth, but also to monitor the deposition of complex structures on a few monolayers scale.

ACKNOWLEDGMENTS

The authors would like to thank Professor J. L. Morenza for helpful discussions and encouragement. This research was supported by the CAICYT of Ministerio de Educación y Ciencia under Contract No. 798/84 and the French/Spanish integrated action No. 176/89. One of the authors (A.C.) acknowledges partial support by CIRIT (AR/88).

[1] R. W. Collins, in *Advances in Amorphous Semiconductors*, edited by H. Fritzsche (World Scientific, Singapore, 1989), p. 1003, and references therein.
[2] B. Drévillon, Thin Solid Films **163**, 157 (1988).
[3] B. Drévillon, J. Non-Cryst. Solids **114**, 139 (1989).
[4] A. M. Antoine, B. Drévillon, and P. Roca i Cabarrocas, J. Appl. Phys. **61**, 2501 (1987).
[5] A. M. Antoine and B. Drévillon, J. Appl. Phys. **63**, 360 (1988).
[6] S. Kumar and B. Drévillon, J. Appl. Phys. **65**, 3023 (1989).
[7] R. W. Collins and J. M. Cavese, J. Non-Cryst. Solids **97&98**, 269 (1987).
[8] B. Drévillon, Thin Solid Films **130**, 165 (1985).
[9] R. W. Collins and B. Y. Yang, J. Vac. Sci. Technol. B **7**, 1155 (1989).
[10] J. L. Andújar, E. Bertran, A. Canillas, J. Esteve, J. Andreu, and J. L. Morenza, Vacuum **39**, 795 (1989).
[11] B. Drévillon, J. Perrin, R. Marbot, A. Violet, and J. L. Dalby, Rev. Sci. Instrum. **53**, 969 (1982).
[12] A. Canillas, E. Bertran, J. L. Andújar, and J. L. Morenza, Vacuum **39**, 785 (1989).
[13] R. M. A. Azzam and N. M. Bashara, in *Ellipsometry and Polarized Light* (North-Holland, Amsterdam, 1977), Chap. 4.
[14] D. A. G. Bruggeman, Ann. Phys. (Leipzig) **24**, 636 (1935).
[15] D. E. Aspnes, Thin Solid Films **89**, 249 (1982).
[16] J. B. Theeten, Surf. Sci. **96**, 275 (1980).
[17] R. W. Collins and J. M. Cavese, J. Appl. Phys. **61**, 1662 (1987).
[18] B. Drévillon, J. Y. Parey, M. Stchakovsky, R. Benferhat, Y. Josserand, and B. Schlayen, SPIE Symp. Proc. **1188**, 174 (1990).